

## Research Article

## Utilization of Tunisian Bentonite as Ion-Exchange and Sorbent Material in The Removal of Lead From Aqueous Solution

Y. Hannachi<sup>a\*</sup> and T.Boubaker<sup>a</sup><sup>a</sup>Laboratory of Heterocyclic Chemistry, Natural Products and Reactivity, Faculty of Sciences of Monastir, 5019 Monastir, Tunisia

Accepted 25 Jan. 2013, Available online 1 March 2013, Vol.3, No.1 (March 2013)

### Abstract

The adsorption characteristics of Pb(II) ions using the Tunisian bentonite were investigated. Experimental parameters affecting the adsorption process such as pH, contact time, adsorbent dosage and temperature were studied. Langmuir, Freundlich and Dubinin–Radushkevich (D–R) models were applied to describe the biosorption isotherms. The adsorption capacity of bentonite for Pb(II) ions was found to be 36.23 mg/g. From the D–R isotherm model, the mean free energy was calculated as 11. kJ/mol, indicating that the adsorption of Pb(II) ions was taken place by ion-exchange process. The calculated thermodynamic parameters showed that the adsorption of Pb(II) ions onto bentonite was feasible, spontaneous and exothermic in nature. Kinetics data were best described by pseudo-second-order model. Infrared (IR) spectra of the bentonite sample showed that the positions and shapes of the fundamental vibrations of the OH and Si–O groups were influenced by the adsorbed Pb(II) cations. The X-ray diffraction (XRD) spectra indicated that the Pb(II) adsorption onto the bentonite samples led to changes in unit cell dimensions and symmetry of the parent bentonite.

**Keywords:** Bentonite, ion-exchange, Langmuir isotherm, pseudo-second-order model, mass transfer analysis, Thermodynamic, (IR) spectra, (XRD) spectra.

### 1. Introduction

Heavy metal pollution is an environmental problem of worldwide concern with effluents from various industrial processes representing one of the most important sources of pollution.

Lead is a highly toxic heavy metal which adversely affects the red blood cells of the human's nervous system and kidneys (Acharya et al., 2009; Potgieter et al., 2006). It has become one of the major environmental pollutants because of its presence in the atmosphere as gases, generated from combustion of fuel lead content, in waters and soils through the effluents of lead smelting, mining and battery manufacturing, paint, paper and pulp industries (Mohan and Pittman, 2006). The current EPA and WHO drinking water standard for lead is 0.05 mg/L and 10 µg/L, respectively (Gupta & Rastogi 2008). Therefore, the reduction of amount of this metal from such effluents to a permissible limit before discharging them into streams and rivers is very important for human health and environment. In this regard, several conventional wastewater treatment technologies such as ion exchange, chemical precipitation, evaporation, membrane filtration, reverse osmosis and electrodialysis were developed and are used successfully (Kiran et al. 2007; Cesur & Baklaya 2007). The main drawbacks of these methods lie with

relatively low treatment efficiency, complicated operation, high cost and possible secondary pollution. In this context, the search for eco-friendly and cost effective new technologies able to remove Pb (II) ions from wastewaters has become a major topic for research. Adsorption compared with other methods appears to be an attractive process in view of its high efficiency, easy handling, availability of different adsorbents and cost effectiveness. Activated carbon in most cases has been used as an adsorbent for reclamation of municipal and industrial wastewater for almost the last few decades (Kandah 2004). But the high cost of activated carbon has inspired investigators, especially in developing countries like Tunisia, to search for suitable low-cost adsorbents.

Among natural adsorbents bentonite occupy a prominent position being low cost, available in abundance and having good sorption properties. Bentonite is the name of the rock that contains the montmorillonite type of clay minerals. Compared with other clay types, montmorillonite has excellent sorption properties and possesses sorption sites available within its interlayer space as well as on the outer surface and edges. Montmorillonite belongs to the 2:1 clay family, the basic structural unit of which is composed of two tetrahedrally coordinated sheets of silicon ions surrounding a sandwiched octahedrally coordinated sheet of aluminum ions. The binding force between the stacked layers of

\*Corresponding author: Y. Hannachi

basic units is mainly the weak van der Waals type of force, which facilitates change in the interlayer space size depending on the humidity conditions and/or the type of material encountered within the interlayer spacing of the clay. Montmorillonite is usually subjected to isomorphous substitution (e.g., substitution of  $Mg^{2+}$  for  $Al^{3+}$ ), thus leading to the development of a negative charge on the entire structure (Tabak et al.2007; Abollino et al.2003).

Adsorption of metal ions onto montmorillonite appears to involve two distinct mechanisms: (i) an ion exchange reaction at permanent charge sites, and (ii) formation of complexes with the surface hydroxyl groups (Ayuso & Sa'nchez 2003).

The present study deals with a series of batch adsorption experiments to investigate and explore the feasibility of bentonite as low cost and readily available adsorbent for removal of

Pb(II) from aqueous solutions. Effect of different parameters such as initial pH, adsorbent dosage, initial metal ion concentration and contact time on the adsorption of Pb(II) were investigated. The rate kinetics of the adsorption of Pb(II) onto bentonite were studied using different kinetic models. Experimental data were fitted to various isotherm equations to determine the best isotherm to correlate the experimental data. Thermodynamics of adsorption process were studied to determine the change in Gibbs free energy, enthalpy and entropy. The sorption energy of adsorption process was also calculated. The XRD and IR spectra were used to characterize and discern the location of Pb (II) cations onto bentonite

## 2. Materials and methods

### 2.1. Materials

The bentonite sample was obtained from Gabés deposit located in southeastern of Tunisia. The raw clay sample was in the clod sized form when first received. Later, it was grounded and washed in deionized water several times at a 1:10 bentonite/water ratio. The mixture was stirred for 5 h and then kept standing overnight, followed by separation, washing and drying at 70 °C.

### 2.2. Characterization procedures

The mineralogical composition of the bentonite was determined from the XRD pattern of the product taken on a Rigaku 2000 automated diffractometer using Ni filtered Cu K $\alpha$  radiation.

The chemical composition of bentonite was measured by X-ray fluorescence Rigaku RIX2000 and was depicted in Table 1.

Table 1. The chemical composition of bentonite

SiO <sub>2</sub>	Al <sub>2</sub> O <sub>3</sub>	CaO	K <sub>2</sub> O	MgO	Fe <sub>2</sub> O <sub>3</sub>	Na <sub>2</sub> O
62.70	20.10	2.29	2.53	3.64	2.16	0.27

IR spectra of the bentonite samples were recorded in the region 4000–400 cm<sup>-1</sup> on a Mattson-1000 FTIR spectrometer at 4 cm<sup>-1</sup> resolution. The surface area was determined by BET method using a surface area analyzer (Model 1750 SORPTY, Carlo Erba, Italy) and was found to be 18.87 m<sup>2</sup>/g. The cation exchange capacity (CEC) of the sample was estimated by using the copper bisethylenediamine complex method (Bergaya & Vayer 1997). The value of CEC for bentonite was 15.87 mg Cu(II) g<sup>-1</sup> bentonite.

### 2.3. Batch sorption experiments

All the necessary chemicals used in the study were of analytical grade. Lead nitrate was obtained from sigma-Aldrich (Ireland). Stock solution of the above heavy metals was made by dissolving exact amount of respective metal salt. The range of concentration of the metal components prepared from stock solution was varied between 3 mg/L to 300 mg/L. The test solutions were prepared by diluting 1 g/L of stock metal solution with double distilled water.

The necessary amount of bentonite was taken in a 250 mL stopper conical flask containing 100 mL of desired concentration of the test solution at the desired pH value. pH of the solution was monitored in a 5500 EUTECH pH Meter using FET solid electrode calibrated with standard buffer solutions by adding 0.1 M HCl and 0.1 M NaOH solution as per required pH value. Necessary amount of bentonite was then added and contents in the flask were shaken for the desired contact time in an electrically thermostated reciprocating shaker @ 120–130 strokes/min at 30 °C. The time required for reaching the equilibrium condition estimated by drawing samples at regular intervals of time till equilibrium was reached. The contents of the flask were filtered through filter paper and the filtrate was analyzed for remaining metal concentration in the sample using Atomic Absorption Spectrophotometer (SHIMADZU AA-680, Japan). The percent adsorption of metal ion was calculated as follows:

$$\text{Adsorption}(\%) = \frac{(C_i - C_f)}{C_i} \times 100 \quad (1)$$

where  $C_i$  and  $C_f$  are the initial and final (or equilibrium) metal concentrations, respectively.

All the investigations were carried out in triplicate to avoid any discrepancy in experimental results with the reproducibility and the relative deviation of the order of  $\pm 0.5\%$  and  $\pm 2.5\%$ , respectively. The effect of pH on adsorption was conducted by batch adsorption process described above maintaining the solution pH adjusted to  $2.0 \pm 0.1$  to  $8.0 \pm 0.1$  under thermostated conditions of 30 °C. The effect of temperature on adsorption isotherm was conducted under isothermal condition at 30 °C, 40 °C and 50 °C where temperature varied within  $\pm 0.5$  °C.

## 3. Results and discussion

3.1. X-ray diffraction studies of the pristine and metal-loaded bentonite

Table 2. *d*-Spacing and relative intensity for bentonite samples

Pristine <i>d</i> (Å)	15.33	4.41	3.80	3.54	3.28	3.03	2.76	2.55	2.19	1.69	1.49
<i>I</i> / <i>I</i> <sub>0</sub>	100	40	10	8	18	16	4	26	6	8	16
Pb loaded <i>d</i> (Å)	13.97	4.48	3.93	3.46	3.31	2.99	2.76	2.57	2.39	1.68	1.49
<i>I</i> / <i>I</i> <sub>0</sub>	100	68	16	18	24	20	8	32	12	8	30

The XRD patterns of the pristine and Pb(II) loaded bentonite are presented in Fig. 1 and the details of their reflection positions and intensities are reported in Table 2.

For the XRD pattern of the pristine bentonite, one reflection was observed in the region  $2^\circ < 2\theta < 8^\circ$ . This corresponds to the  $5.76^\circ$  ( $2\theta$ ) value from which the interlamellar distance was found to be 15.33 Å (Fig. 1.a). However, several reflections were observed in the region  $2^\circ < 2\theta < 8^\circ$  for the pattern of the Pb(II) saturated bentonite sample (Fig. 1.b). One reflection situated at a higher  $2\theta$  value corresponds to the basal spacing, the other reflections situated at a lower  $2\theta$  values are likely to appear because of the agglomeration of clay sheets (Dermatas & Dadachov 2003). The adsorption of Pb(II) onto the bentonite led to decrease in the basal space of the host material from 15.33 to 13.97 Å. The intensity gain in and Pb loaded bentonite is approximately 1.33 fold higher than in its host material counterpart. The differences of XRD patterns of the pristine and metal-loaded bentonite indicate the effects of Pb(II) adsorption on the structure of clay mineral, and are not sample-specific.

The XRD spectra of Pb- loaded bentonite indicated that the Pb(II) adsorption may lead to changes in unit cell dimensions and symmetry of the parent bentonite. Also, the Bragg angle for several reflections has notably changed, while for others it essentially remained same. These findings show that Pb(II) cations are arranged in one or more equivalent positions and they contribute to the reflection intensities.

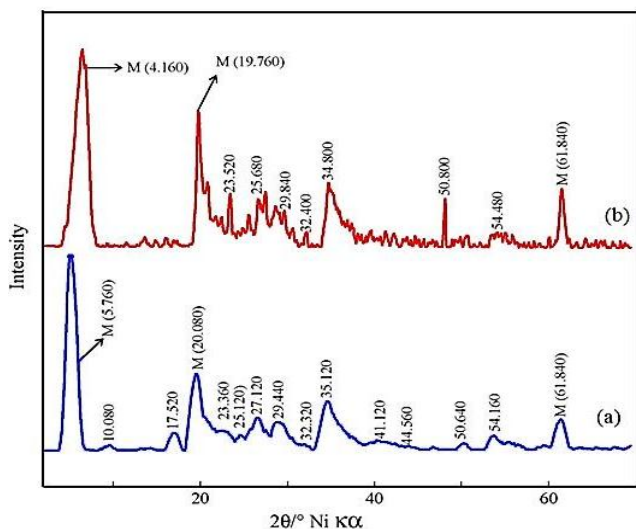


Fig. 1. The XRD patterns of the pristine (a) and Pb(II) loaded bentonite (b) (M: montmorillonite).

### 3.2. IR spectra studies of the pristine and metal-loaded bentonite

The XRD and IR spectra of bentonite indicate that montmorillonite is the dominant mineral phase in this clay (Figs. 1a and 2a).

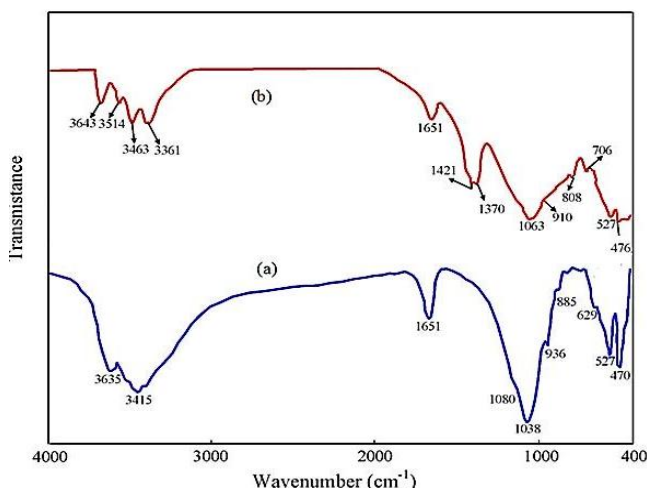


Fig.2. IR spectra of the pristine (a) and Pb(II) loaded bentonite (b)

The absorption band at  $3635\text{ cm}^{-1}$  is due to stretching vibrations of structural OH groups of montmorillonite. The bands corresponding to AlAlOH, AlFeOH and AlMgOH bending vibrations were observed at 936, 885 and  $845\text{ cm}^{-1}$ , respectively. A complex band at  $1038\text{ cm}^{-1}$  is related to the stretching vibrations of Si–O groups, while the bands at 527 and  $470\text{ cm}^{-1}$  are due to Al–O–Si and Si–O–Si bending vibrations, respectively. The band at  $629\text{ cm}^{-1}$  was assigned to coupled Al–O and Si–O out-of-plane vibrations. Water in montmorillonite gave a broad band at  $3415\text{ cm}^{-1}$  corresponding to the H<sub>2</sub>O-stretching vibrations, with a shoulder near  $3330\text{ cm}^{-1}$ , due to an overtone of the bending vibration of water observed at  $1651\text{ cm}^{-1}$  (Madejová 2003). Detailed analysis of IR spectra in the whole spectral region (4000–400  $\text{cm}^{-1}$ ) can be used for discerning the location of Pb(II) cations. The structural modifications of the tetrahedral and octahedral sheets due to the adsorbed Pb(II) ions influenced the fundamental vibrations of the Si–O and OH groups (Fig. 2b). For example, the stretching OH band was shifted up to  $3643\text{ cm}^{-1}$  and moreover, a new band appeared near  $3514\text{ cm}^{-1}$  in the spectrum of Pb(II)-saturated bentonite sample. This band, assigned to AlMgPbOH vibration, confirms the presence of the Pb(II) ions in the former vacant octahedral sites. The IR pattern of the Pb(II)-

saturated bentonite sample showed a strong broad band of water near  $3463\text{ cm}^{-1}$ , due to the overlapping asymmetric  $\nu_3$  and symmetric  $\nu_1$  (H–O–H) stretching vibrations and the absorption near  $1635\text{ cm}^{-1}$  related to the  $\nu_2$  (H–O–H) bending vibrations. The band of RB at  $3361\text{ cm}^{-1}$  was ascribed to an overtone ( $2\nu_2$ ) of the bending mode (Bishop & Pieters 1994). The broad band near  $1038\text{ cm}^{-1}$ , assigned to complex Si–O stretching vibrations in the tetrahedral sheet, upon saturation process moved to  $1049\text{ cm}^{-1}$  for the pristine bentonite sample. The position of the Si–O bending vibration at  $527\text{ cm}^{-1}$ , due to Si–O–Al remained basically unchanged for the Pb(II)-loaded sample, but some broadening and a decrease in intensity of the Si–O–Al band were observed.

### 3.3. Effect of pH

pH has a significant impact on heavy metal removal by bentonite since it can influence both the adsorbent surface metal binding sites and the metal chemistry in water. To examine the effect of pH on the lead ions removal efficiency, several experiments were performed at different pH ranges from 2 to 8 as shown in Fig. 3.

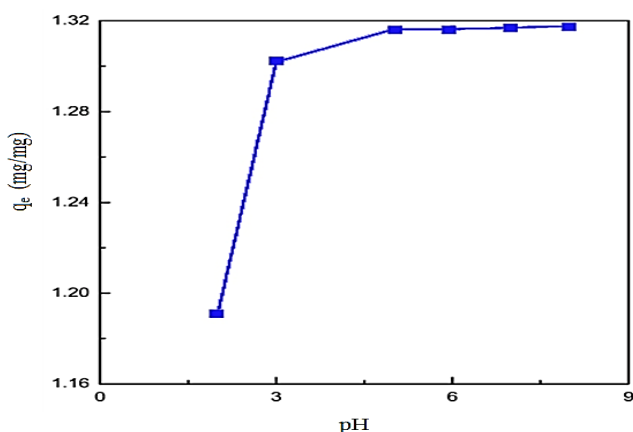


Fig. 3. Effect of pH (metal concentration 25 mg/L; adsorbent dosage 7.5 g/L, contact time 2 h)

The adsorption efficiency increased with increasing the pH value and reaches a plateau at a pH value of 5. Under acidic conditions, the adsorption capacity of bentonite is low because of the dissolution of  $\text{Al}^{3+}$  ions from the aluminosilicate layers and the competition between the protons ( $\text{H}^+$ ) and metal ions ( $\text{Pb(II)}$ ) for the exchange sites on the bentonite particle. However, with increasing pH, the competition from the hydrogen ions decreases and the positively charged  $\text{Pb(II)}$  ions can be exchanged with exchangeable cations and can also be adsorbed at the negatively charged sites on the bentonite. To ensure the interference from metal precipitation, subsequent experiments were carried out at pH 5.

### 3.4. Effect of adsorbent concentration

The effect of adsorbent dosage in terms of removal efficiency (mg/g of adsorbent dosage) on the removal of metal ion is represented in Fig. 4.

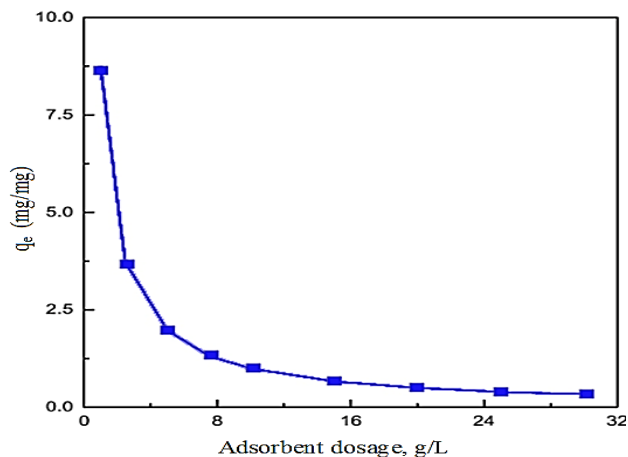


Fig. 4. Effect of bentonite concentration on adsorption of Pb(II) (pH 5, metal concentration 10 mg/L, contact time 2 h.)

For higher adsorbent dosage particularly after adsorbent dosage level of 7.5 g/L, the incremental metal ion removal becomes very low as the surface metal ion concentration and the solution metal ion concentration comes to equilibrium with each other.

### 3.5. Effect of initial metal ion concentration

Effect of initial metal ion concentration in terms of distribution co-efficient  $K_d$ , as stated in Eq. (2) is shown in Fig. 5.

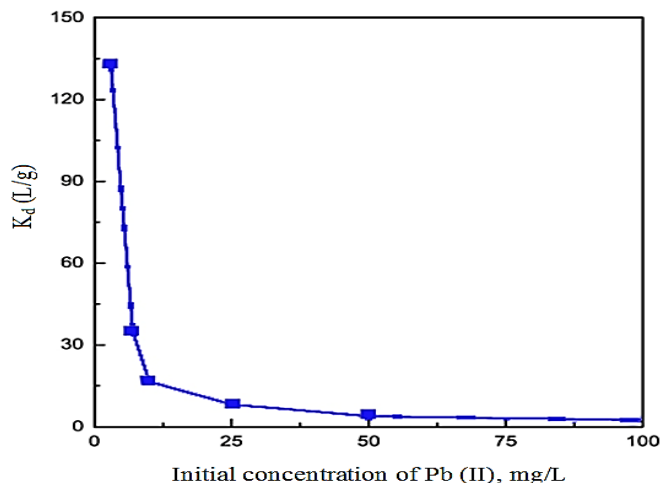


Fig.5. Effect of initial concentration on the adsorption of Pb(II) pH 5, adsorbent concentration. 5 g/L, contact time 2 h.

$$K_d = \frac{(C_0 - C_e)}{C_e} \left( \frac{V}{M} \right) \tag{2}$$

where  $C_0$  and  $C_e$  are the initial and equilibrium metal concentrations, respectively,  $V$  is the volume of the solution (mL) and  $M$  is the metal ion.

The  $K_d$  values increase with the decreasing concentration of metal ion. In other words  $K_d$  values increase as the

dilution of metal ion proceeds. This effect can be explained as at low metal ion/adsorbent ratios, metal ion adsorption involves higher energy sites. As the metal ion/adsorbent ratio increases, the higher energy sites are saturated and adsorption begins on lower energy sites, resulting in decreases in the removal of metal ion.

### 3.6. Effect of contact time and adsorption rate kinetics mechanism

The studies were carried out by conducting the experimental runs measuring the effect of contact time on the batch adsorption of metal solution containing 10 mg/L of Pb(II) at 30 °C and initial pH value of 5. The adsorption yields increase with contact time and attain a maximum value at certain contact time, thereafter, it remains almost constant. At these points the adsorbents surfaces are saturated with metal ions. In present studies, for Pb(II) equilibrium was achieved by 2 h of contact time.

### 3.7. Adsorption kinetics study

The study of adsorption kinetics describes the solute uptake rate and evidently these rate controls the residence time of adsorbate uptake at the solid–solution interface including the diffusion process. The mechanism of adsorption depends on the physical and chemical characteristics of the adsorbent as well as on the mass transfer process (Metcalf 2003). The results obtained from the experiments were used to study the kinetics of metal ion adsorption.

The rate kinetics of metal ion adsorption on bentonite was analyzed using pseudo-first order (Lagergren 1898), pseudo-second order (Ho et al.2000), and intraparticle diffusion models (Weber & Morris 1963). The conformity between experimental data and the model predicted values was expressed by correlation coefficients ( $r^2$ ) as well as Chi square ( $\chi_t^2$ ) value.

#### 3.7.1. Lagergren model

The linearized form of the pseudo-first-order rate equation by Lagergren is given as:

$$\log(q_e - q) = \log q_e - \frac{K_{ad}t}{2.303} \tag{3}$$

where  $q$  and  $q_e$  (mg/g) are the amounts of the metal ions adsorbed at equilibrium (mg/g) and  $t$  (min), respectively and  $k_{ad}$  is the rate constant of the equation ( $\text{min}^{-1}$ ). The adsorption rate constants ( $k_{ad}$ ) can be determined experimentally by plotting of  $\log(q_e - q)$  versus  $t$ .

#### 3.7.2. Pseudo-second order model

Experimental data were also tested by the pseudo-second order kinetic model which is given in the following form:

$$\frac{t}{q} = \frac{1}{k_2 q_2^2} + \frac{t}{q_2} \tag{4}$$

where  $k_2$  ( $\text{gmg}^{-1} \text{min}^{-1}$ ) is the rate constant of adsorption,  $q_2$  is maximum adsorption capacity ( $\text{mg g}^{-1}$ ). The values of  $k_2$ ,  $q_2$  were obtained from the slopes and intercepts of plots of  $t/q_t$  versus  $t$  at different temperatures. This model is more likely to predict kinetic behavior of adsorption with chemical sorption being the rate-controlling step.

#### 3.7.3. Intraparticle diffusion model

The intraparticle diffusion model (Fig. 6) is based on the theory proposed by Weber and Morris. According to this theory

$$q = K_t t^{0.5} \tag{5}$$

where  $q$  is the amount adsorbed per g of the adsorbent (mg/g),  $K_t$  is the intra-particle rate constant [ $(\text{mg/g min}^{1/2})$ ] and  $t$  is the time (min).

In order to quantify the applicability of each model, the correlation coefficients,  $r^2$ , was calculated from these plots. The linearity of these plots indicates the applicability of the three models.

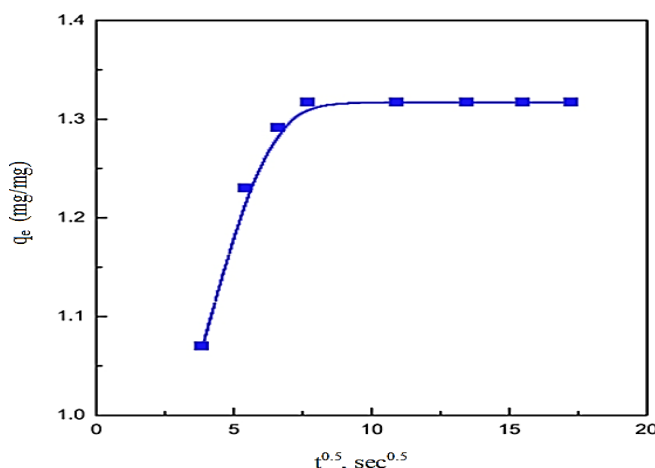


Fig.6. Intraparticle diffusion plot for the adsorption of Pb(II) by bentonite( pH 5, metal concentration 10 m/L, and adsorbent dosage 7.5 g/L, temperature 30 °C)

The values of rate constants and correlation coefficients for each model are shown in Table 3. However, the correlation coefficients,  $r^2$ , showed that the pseudo-second order model, an indication of chemisorptions mechanism, fits better with the experimental data than the pseudo-first order model. In addition, the Chi-square test was also carried out to support the best fit adsorption model. The equation for evaluating the best fit model is to be written as:

$$\chi_t^2 = \sum \frac{(q_t - q_{tm})^2}{q_{tm}} \tag{6}$$

It has been found that  $\chi_t^2$  values are much less in pseudo-second order model than that of pseudo-first order and intraparticle diffusion model. Thus based on the high correlation coefficient and low  $\chi_t^2$  value, it can be said that adsorption of Pb(II) onto bentonite follows pseudo-second order model than that of intraparticle diffusion model.

Table 3. Rate kinetics for adsorption of Pb(II) by bentonite

Lagergreen 1st order			Pseudo- second order			Weber and Morris		
$K_{ad} \times 10^{-2} \text{ (min}^{-1})$	$r^2$	$\chi^2$	$K_2 \text{ (g/mg min)}$	$r^2$	$\chi^2$	$K_i \times 10^{-2} \text{ (mg/g min}^{1/2})$	$r^2$	$\chi^2$
7.37	0.998	2.045	1.606	0.9992	0.0269	6.4	0.93	1.18

3.7.4. Mass transfer analysis

Mass transfer analysis for the removal of Pb(II) from aqueous solutions by bentonite was carried out using the following equation (McKay et al.1981) :

$$\ln\left(\frac{C_t}{C_0} - \frac{1}{1+MK_{bq}}\right) = \ln\left(\frac{MK_{bq}}{1+MK_{bq}}\right) - \left(\frac{1+MK_{bq}}{MK_{bq}}\right)\beta S_s t \tag{7}$$

where C0 is the initial concentration of metal ion in solution (mg/L), Ct is the concentration of metal ion in solution after time t (mg/L), K<sub>bq</sub> is the constant obtained by multiplying q<sub>max</sub> and b, M is the mass of the adsorbent per unit volume (g/L), S<sub>s</sub> is the external surface area of the adsorbent per unit volume (m<sup>-1</sup>) and β is the mass transfer coefficient (m/s).

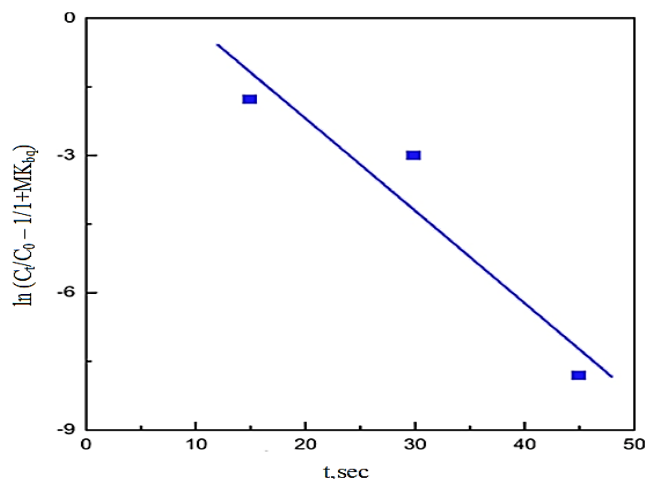


Fig. 7. Mass transfer analysis for the adsorption of Pb(II) by bentonite (pH 5, metal concentration 10 mg/L, and adsorbent dosage 7.5 g/L, temperature 30 °C.)

The plot of

$$\ln\left(\frac{C_t}{C_0} - \frac{1}{1+MK_{bq}}\right)$$

versus t results a straight line (Fig. 7) of slope

$$\left(\frac{1+MK_{bq}}{MK_{bq}}\right)\beta S_s$$

and the values of mass transfer coefficients (β) calculated from the slops of the plots were 2.514 × 10<sup>-5</sup> cm/s with a high value of correlation coefficient. The values of mass transfer coefficients (β) obtained from the study indicate

that the transport of the adsorbate from bulk to the solid phase was quite fast.

3.8. Adsorption isotherms

The adsorption isotherm for the removal of metal ion was studied using initial concentration of between 10 and 300 mg/L at an adsorbent dosage level of 7.5 g/L for Pb(II) 30 °C. The adsorption equilibrium data are conveniently represented by adsorption isotherms, which correspond to the relationship between the mass of the solute adsorbed per unit mass of adsorbent q<sub>e</sub> and the solute concentration for the solution at equilibrium C<sub>e</sub>.

3.8.1. Langmuir and Freundlich adsorption isotherm models

To model the experimental equilibrium data, the Langmuir and Freundlich isotherm models were used. The theoretical Langmuir adsorption isotherm model is best known to all the isotherm models, and describes the adsorption of a solute from a liquid solution.

Langmuir adsorption isotherm (Langmuir 1918) applied to equilibrium adsorption assuming mono-layer adsorption onto a surface with a finite number of identical sites and is represented as follows:

$$\frac{C_e}{q_e} = \frac{1}{q_{\infty} b} + \frac{C_e}{q_{\infty}} \tag{8}$$

where q<sub>e</sub> is the equilibrium metal ion concentration on the adsorbent (mg/g), C<sub>e</sub> is the equilibrium metal ion concentration in the solution (mg/L), q<sub>max</sub> is the monolayer adsorption capacity of the adsorbent (mg/g), and b is the Langmuir adsorption constant (L/mg) relating the free energy of adsorption. Linear plots of C<sub>e</sub>/q<sub>e</sub> vs C<sub>e</sub> (Fig. 8) were employed to determine the value of q<sub>max</sub> (mg/g) and b (L/mg). The data obtained with the correlation coefficients (r<sup>2</sup>) were listed in Table 4.

The Freundlich adsorption isotherm is an empirical equation based on the adsorption on the heterogeneous surface. The linear form of the Freundlich adsorption isotherm can be defined by the following equation (Freundlich, 1906):

$$\log q_e = \log k_f + \frac{1}{n} \log C_e \tag{9}$$

The Freundlich isotherm constant n is an empirical parameter that varies with the degree of heterogeneity and

Table 4. Langmuir and Freundlich adsorption isotherm constants for Pb(II) adsorption onto bentonite

Langmuir constants				Freundlich constants			
$q_{max}$ (mg/mg)	b	$r^2$	$\chi^2$	$K_f$ (mg/g)/(mg/L) <sup>1/n</sup>	n	$r^2$	$\chi^2$
36.23	0.14	0.994	1.184	4.37	1.77	0.991	1.475

$k_f$  is related to adsorption capacity. The constants  $k_f$  and  $n$  were calculated from Eq. (9) and Freundlich plots. The

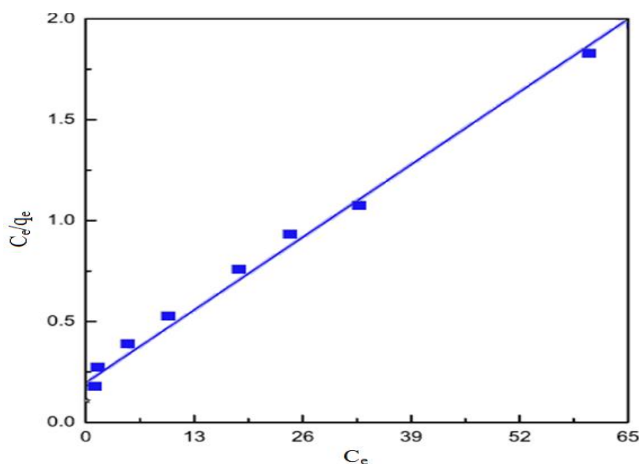


Fig. 8. Langmuir plot for the adsorption of Pb(II) by bentonite pH 5, adsorbent dosage, 7.5 g/L; contact time 2 h and temperature 30 °C.

amount of adsorbent required to reduce any initial concentration to predetermined final concentration can be calculated. The values for Freundlich constants and correlation coefficients ( $r^2$ ) for the adsorption process are also presented in Table 4.

The values of  $n$  between 1 and 10 (i.e.  $1/n$  less than 1) represent a favorable adsorption. The values of  $n$ , which reflect the intensity of adsorption, also reflected the same trend. The  $n$  values obtained for the adsorption process represented a beneficial adsorption. Table 4 shows that the experimental data are better fitted to Langmuir ( $r^2 = 0.9986$ ) than Freundlich ( $r^2 = 0.9903$ ) adsorption isotherm. Moreover Chi-square ( $\chi^2$ ) test also confirms the fact. Therefore uptake of Pb(II) ion preferably follows the monolayer adsorption process.

### 3.8.2. Dubinin–Radushkevich (DR) isotherm

The equilibrium data were also subjected to the Dubinin–Radushkevich (D–R) isotherm model to determine the nature of adsorption processes as physical or chemical. The D–R sorption isotherm is more general than Langmuir isotherm, as its derivation is not based on ideal assumptions such as equipotent of the sorption sites, absence of steric hindrance between sorbed and incoming particles and surface homogeneity on microscopic level (Malik et al. 2005). The linear presentation of the D–R isotherm equation (Dubinin et al. 1947) is expressed by:

$$\ln q_e = \ln q_m - \beta \varepsilon^2 \tag{10}$$

where  $q_e$  is the amount of metal ions adsorbed on per unit weight of adsorbent (mol/L),  $q_m$  is the maximum adsorption capacity (mol/g),  $\beta$  is the activity coefficient related to adsorption mean free energy (mol<sup>2</sup>/J<sup>2</sup>) and  $\varepsilon$  is the Polanyi potential

$$\varepsilon = RT \ln \left( 1 + \frac{1}{C_e} \right)$$

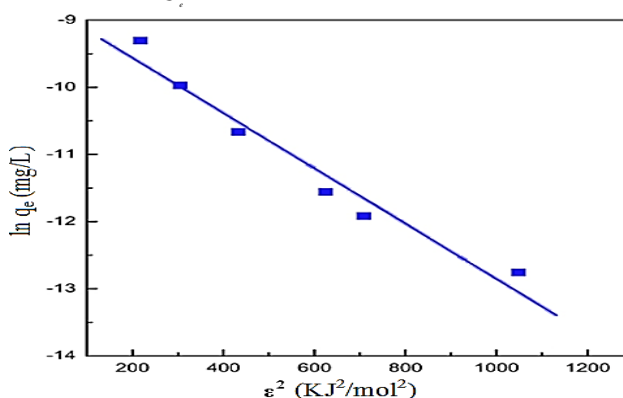


Fig.9. D–R isotherm plots for adsorption of Pb(II) onto bentonite ( adsorbent dosage 7.5 g/L; contact time 2 h; pH 5; temperature 30°C).

Fig. 9 shows the plot of  $\ln q_e$  vs  $\varepsilon^2$  is a straight line from which values of  $\beta$  and  $q_m$  for Pb(II) were evaluated. Using the calculated value of  $\beta$ , it was possible to evaluate the mean sorption energy,  $E$ , from

$$E = \frac{1}{\sqrt{-2\beta}} \tag{11}$$

The  $E$  (kJ/mol) value gives information about adsorption mechanism, physical, ion-exchange or chemical. If it lies between 8 and 16 kJ/mol, the adsorption process takes by ion-exchange and while  $E < 8$  kJ/mol, the adsorption process proceeds physically (Helfferich 1962). The mean adsorption energy was calculated as 11 kJ/mol for the adsorption of Pb(II) ions. This result indicated that the adsorption process of Pb (II) ions onto bentonite was taken place by ion-exchange.

### 3.9. Adsorption thermodynamics

#### 3.9.1. Effect of temperature on adsorption of Pb(II)

Adsorption experiments to study the effect of temperature were carried out at 30, 40 and 50°C at optimum pH value of 5 and adsorbent dosage level of 7.5 g/L. The

equilibrium contact time for adsorption was maintained at 2 h. The percentage of adsorption decreases with rise of temperature from 30 to 50 °C. The results were shown in Table 5 and it revealed the exothermic nature of the adsorption process which later utilized for determination of changes in Gibbs free energy  $\Delta G$ , heat of adsorption  $\Delta H$  and entropy  $\Delta S$  of the adsorption of Pb(II) from aqueous solutions.

Table 5. Effect of temperature on the adsorption of Pb(II) onto bentonite

Temperature (°C)	% Removal of Pb (II) at initial metal ion concentration		
	10	25 mg/L	50 mg/ L
30	98.63	97.84	96.25
40	97.71	96.72	94.63
50	96.54	96.42	93.72

The decrease in adsorption with rise in temperature may be due to the weakening of adsorptive forces between the active sites of the adsorbent and adsorbate species and also between the adjacent molecules of the adsorbed phase.

3.10.2. Effect of temperature on thermodynamics parameter on adsorption of Pb(II)

The variation in the extent of adsorption with respect to temperature has been explained on the basis of thermodynamic parameters viz. changes in standard free energy, enthalpy and entropy. The dependence on temperature of adsorption of Pb(II) onto bentonite was evaluated using equations:

$$\ln k_c = \frac{\Delta S}{R} - \frac{\Delta H}{RT} \tag{12}$$

(Van't Hoff equation)

$$\Delta G^\circ = -RT \ln k_c \tag{13}$$

where  $K_c = (q_e/C_e)$  is the adsorption equilibrium constant,  $T$  is absolute temperature (K),  $R$  is gas constant. When  $\ln Kc$  versus  $1/T$  is plotted (Fig.10),  $\Delta H$  and  $\Delta S$  values can be computed from slope and intercept of the van't Hoff equation.

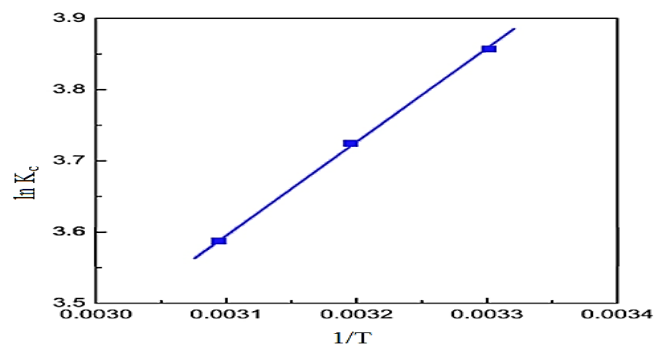


Fig.10. Plot of  $\ln K_c$  vs.  $1/T$  for the estimation of thermodynamic parameters for adsorption of Pb(II) onto bentonite

The calculated parameters were given in Table 6. It may be concluded from the negative values of  $\Delta H$  and  $\Delta G$  that the sorption process is exothermic and spontaneous.

Table.6. Thermodynamic parameters for Pb (II) adsorption onto bentonite

$\Delta H$ (kJ/mol)	$\Delta S$ (kJ/mol)	T (k)	- $\Delta G$ (kJ/mol)	$r^2$
-25.741	-0.0504	303	10.62	0.9275
		313	9.693	
		323	9.632	

The negative  $\Delta S^\circ$  value means a decrease in the randomness at the solid/solution interface during the adsorption process (Dekhil et al.2011)

Conclusions

In this study, the use of bentonite as an adsorbent was tested for removing of Pb(II) ions from aqueous solution. The batch study parameters, pH of solution, adsorbent concentration, contact time, and temperature, were found to be effective on the adsorption efficiency of Pb(II) . The adsorption capacity of bentonite was determined as 36.23 mg/g. at optimum conditions of pH 5, contact time of 120min and temperature of 30 °C. The mean free energy value evaluated from the D–R model indicated that the adsorption of Pb(II) onto bentonite was taken place by ion-exchange process. Experimental data obtained from rate kinetics were better described by pseudo-second order model than pseudo-first order model as evident from correlation co-efficient values ( $r^2$ ) and  $x_t^2$  . The calculated thermodynamic parameters showed the feasibility, exothermic and spontaneous nature of the adsorption of Pb(II) ions onto bentonite. The X-ray diffraction (XRD) spectra indicated that the Pb(II) adsorption onto the bentonite samples led to changes in unit cell dimensions and symmetry of the parent bentonite. Infrared (IR) spectra of the bentonite sample showed that the positions and shapes of the fundamental vibrations of the OH and Si–O groups were influenced by the adsorbed Pb(II) cations. The findings of this study revealed that bentonite is an effective and alternative adsorbent for the removal of Pb(II) ions from aqueous solution because of its considerable ion exchange capacity, being of natural, renewable and thus cost-effective adsorbent.

References

Abollino, O., Aceto, M., Malandrino, M., Sarzanini, C and Mentasti, E.(2003). Adsorption of heavy metals on Namontmorillonite, Effect of pH and organic substances, Water Research 37:1619–1627.  
 Acharya, J., Sahu, J. N., Mohanty, C. R. and Meikap, B. C. (2009). Removal of lead(II) from wastewater by activated carbon developed from Tamarind wood by zinc chloride activation. Chemical Engineering Journal 149: 249- 262.

- Ayuso, E. A. and Sanchez, A. G. (2003). Removal of heavy metals from waste waters by natural and Na-exchanged bentonites, *Clays and Clay Minerals* **51**: 475–480.
- Bergaya, F. and Vayer, M. (1997). CEC of clays: measurement by adsorption of a copper ethylenediamine complex. *Applied Clay Science* **12**: 275–280.
- Bishop, J.L., Pieters, C.M and Edwards, J.O. (1994). Infrared spectroscopic analyses on the nature of water in montmorillonite, *Clays and Clay Minerals* **42**: 702–716.
- Cesur, H. and Baklaya, N. (2007). Zinc removal from aqueous solution using an industrial by-product phosphogypsum, *Chemical Engineering Journal* **131**: 203–208.
- Dekhil, A. B., Hannachi, Y., Ghorbel, A. and Boubaker, T. (2011). Removal of Lead and Cadmium Ions From Aqueous Solutions Using Dried Marine Green Macroalga (*Caulerpa racemosa*). *International Journal of Environmental Research* **5** : 725-732
- Dermatas, D and Dadachov, M.S. (2003). Rietveld quantification of montmorillonites in lead-contaminated soils, *Applied Clay Science* **23**: 245–255.
- Dubin, M.M., Zaverina, E.D., Radushkevich, L.V. (1947). Sorption and structure of active carbons. I. Adsorption of organic vapors, *Zhurnal Fizicheskoi Khimii* **21**: 1351–1362.
- Freundlich, H.M.F., (1906). Adsorption in solution, *Physical Chemistry Chemical Physics* **40** : 1361-1368.
- Gupta, V.K. and Rastogi, A. (2008). Biosorption of lead from aqueous solutions by green algae *Spirogyra* species : Kinetics and equilibrium studies . *The Journal of Hazardous Materials* **152**: 407-414.
- Helferich, F. (1962). *Ion Exchange*, McGraw Hill, NY, USA, 166.
- Ho, Y.S., McKay, G., Wase, D. J and Foster, C.F., (2000). Study of the sorption of divalent metal ions onto peat, *Adsorption Science & Technology* **18** : 639-650
- Kandah, M. I. (2004). Zinc and cadmium adsorption on low-grade phosphate. *Separation and Purification Technology* **35**: 61–70.
- Kiran, B., Kaushik, A. and Kaushik, C. P. (2007). Response surface methodological approach for optimizing removal of Cr (VI) from aqueous solution using immobilized cyanobacterium. *Chemical Engineering Journal* **126**: 147-153 .
- Lagergren, S. (1989). Zur theorie der sogenannten adsorption gelöster stoffe. *Kunglia a svenska venten skapasa kademiens. Hand lingar* **24**: 1-39.
- Langmuir, I., (1918). The adsorption of gases on plane surface of glass, mica and platinum. *Journal of the American Chemical Society* **40**: 1361-1403.
- Madejová, J. (2003). FTIR techniques in clay mineral studies, *Vibrational Spectroscopy* **31**: 1–10.
- Malik, U.R., Hasany, S.M. and Subhani, M.S. (2005). Sportive potential of sunflower stem for Cr(III) ions from aqueous solutions and its kinetic and thermodynamic profile, *Talanta*, **6** : 166–173.
- McKay, G., Otterburn, M.S and Sweeney, A.C. (1981). Surface mass transfer processes during colour removal from effluent using silica *Water Research*, **15**: 327–331.
- Metcalf, E. (2003). *Inc., Wastewater Engineering, Treatment and Reuse*, fourth ed., Tata McGraw–Hill Publishing Company Limited, New Delhi.
- Mohan, D. and Pittman, C. U. (2006). Activated carbons and low cost adsorbents for remediation of tri- and hexavalent chromium from water. *The Journal of Hazardous Materials* **137**: 762 -811.
- Potgieter, J. H., Potgieter, V. S.S. and Kalibantonga, P.D. (2006). Heavy metals removal from solution by palygorskite. *Clay Minerals Engineering* **19**: 463-470.
- Tabak, A., Afsin, B., Aygun, S.F. and Koksal, E. (2007). Structural characteristics of organo-modified bentonites of different origin, *Journal of Thermal Analysis and Calorimetry*, **87**: 375–381.
- Weber, W.J and Morris, J.C.. (1963). Kinetics of adsorption on carbon from solution. *Journal. Sanitary Engineering Division. ASCE*, **89**: 31–59.